

# Numerical study of the influence of forcing terms and fluctuations near onset on the roll pattern in Rayleigh-Bénard convection in a simple fluid

Jorge Viñals

*Supercomputer Computations Research Institute, B-186, Florida State University, Tallahassee, Florida 32306-4052*

Hao-Wen Xi and J. D. Gunton

*Department of Physics, Lehigh University, Bethlehem, Pennsylvania 18015*

(Received 10 December 1991)

The stochastic Swift-Hohenberg equation is studied as a model of Rayleigh-Bénard convection in a simple fluid. The equation has been solved numerically in two spatial dimensions to obtain the convective heat current and the roll pattern when either a bulk stochastic forcing field or different models of thermal-diffusivity mismatch at the sidewalls of the convective cell are considered. The parameters that enter the equation have been chosen to match the ramping experiments on Rayleigh-Bénard convection by Meyer, Ahlers, and Cannell [Phys. Rev. Lett. **59**, 1577 (1987)]. For any combination of forcing mechanisms, we are able to find values of their various amplitudes that lead to excellent fits to the experimentally measured convective current. In the case of a bulk random forcing field, we find an amplitude of  $F_1 = 5 \times 10^{-5}$ , compared to  $F_{th} = 1.92 \times 10^{-9}$ , the value obtained from fluctuation theory. A random, cellular pattern of rolls is observed, in agreement with experiments involving a gel sidewall designed to eliminate the influence of the sidewalls on the onset of convection. A thermal-conductivity mismatch at the sidewall has also been modeled by a variety of forcing fields. In all cases a roll-like pattern that reflects the geometry of the sidewalls is observed. Different combinations of both types of forcing fields have also been studied and found to yield patterns intermediate between cellular and roll-like, while yielding a very reasonable fit to the convective heat current measured experimentally.

PACS number(s): 47.20.Ky, 47.20.Hw, 05.40.+j, 47.25.Qv

## I. INTRODUCTION

Consider a layer of fluid contained within two horizontal parallel plates such that their lateral dimensions are much larger than the width of the layer. If the lower plate is kept at a higher temperature than the upper plate, an initially quiescent conducting state can be driven into a convecting state. The transition occurs when the temperature gradient reaches a critical value at which the internal kinetic energy dissipated by viscosity is no longer sufficient to sustain the internal energy released by the buoyant force. This is the classical Rayleigh-Bénard instability.

In an ideal infinite system, convective motion is triggered by the existing thermal fluctuations in the fluid. At the instability or bifurcation point, thermal fluctuations do not decay but are amplified and lead to macroscopic motion in the whole system. From a theoretical point of view, fluctuations of a hydrodynamic nature can be described along the lines of the classical work of Landau and Lifshitz [1-3]. Experimentally, however, thermal diffusivity mismatches at the sidewalls of the experimental cell or other imperfections in the experimental setup often lead to imperfect bifurcations and hence the role played by the underlying thermal fluctuations at the onset of the instability is difficult to establish.

Recently, Meyer, Ahlers, and Cannell [5-7] have performed a number of experimental studies aimed at elucidating the role of thermal fluctuations on the instabil-

ity. When the working fluid is water and the convection cell is enclosed by a high-density polyethylene sidewall, convective motion is seen to start in the fluid adjacent to the sidewalls and then propagate into the bulk fluid. The pattern is composed of parallel rolls which reflect the geometry of the convection cell. This observation is attributed to a thermal diffusivity mismatch between the fluid and the sidewall which results in temperature gradients normal to the sidewall and in the concomitant heat loss through the wall. Such an effect has been studied theoretically by considering appropriate boundary conditions for the velocity and temperature fields in the hydrodynamic equations of motion for the case of a ramping experiment with stress-free horizontal boundaries [8]. It has been shown that a thermal diffusivity mismatch in the sidewall region can be incorporated in the equation for the envelope function that describes the slow modulations of the roll pattern (often called amplitude equation). Its effect can be modeled as an inhomogeneous boundary condition on the envelope function or as a uniform bulk forcing field on an envelope function that satisfies homogeneous boundary conditions.

When the convection cell is enclosed by a gel sidewall with a thermal diffusivity very similar to that of water [5-7], a random, cellular pattern appears throughout the cell, with no relation to the cell's geometry. Furthermore, the emerging pattern is irreproducible from experiment to experiment. Meyer, Ahlers, and Cannell conclude that the appearance of rolls inside the cell in this case is in no way related to the influence of the sidewalls, hence

the pattern observed should have originated from the underlying thermal fluctuations in the fluid. From the measured convective heat current, a fit to an amplitude equation is used to extract the amplitude of the fluctuations at onset. Quite surprisingly, they find that the amplitude of the fluctuations needed to fit the measured convective current is several orders of magnitude larger than classical thermal fluctuations. As yet, there is no explanation for this observation.

Following earlier work on the subject, we study in this paper the Swift-Hohenberg equation in two spatial dimensions. This equation is believed to have the same long-distance behavior as the Boussinesq approximation to the fluid equations that describe the onset of convection in a simple fluid (the equivalency between both descriptions has only been established for infinite systems and near onset). A great deal of analytical and numerical work on the Swift-Hohenberg equation has already been done by Cross [9, 10], and by Greenside and co-workers [11]. A preliminary account of the research described in this paper was presented elsewhere [12]. We focus in this paper on a numerical investigation of the *stochastic* Swift-Hohenberg equation in two spatial dimensions. We wish to investigate the effect of both the forcing mechanism and the amplitude of bulk fluctuations on the pattern of rolls that emerges after the instability in an effort to clarify the experiments of Meyer, Ahlers, and Cannell. Previous attempts in this direction were based on an amplitude equation description [8, 13] and therefore had no access to the spatial structure of the pattern. In our case, however, any assumption about the structure of the pattern of rolls is not needed.

All the parameters that enter the Swift-Hohenberg equation can be determined for the experiments of Meyer, Ahlers, and Cannell (except for the amplitude of the forcing term). Unfortunately, the equivalence between the Swift-Hohenberg equation and the Boussinesq approximation for a simple fluid has only been established for bulk systems. We know of no derivation of the boundary conditions for the order parameter  $\psi(\mathbf{r}, t)$  in the equation that models lateral heat losses in the fluid. We introduce in this paper a number of phenomenological forcing fields that model this lateral thermal gradient. The simplest one involves introducing a constant bulk forcing field in the equation while retaining homogeneous boundary conditions. In analogy with the work of Ahlers *et al.* [8], we also model the effect of lateral thermal gradients by a forcing field localized in the boundary region in order to mimic an inhomogeneous boundary condition. As we will show later, however, our results concerning the extrapolated amplitude of the fluctuations at onset are fully consistent with previous estimates based on the amplitude equation.

## II. THE SWIFT-HOHENBERG EQUATION

### A. Description of the equation

The Swift-Hohenberg equation describes the evolution of a real order parameter  $\psi(\mathbf{r}, t)$  in two spatial dimensions [3, 4],

$$\frac{\partial \psi}{\partial t} = \frac{1}{\tau_0} \left[ \epsilon(t) - \frac{\xi_0^2}{4q_c^2} (\nabla^2 + q_c^2)^2 - g_3 \psi^2 - g_5 \psi^4 \right] \psi + f(\mathbf{r}, t), \quad (1)$$

where  $\epsilon$  is the reduced Rayleigh number,

$$\epsilon(t) = \frac{R(t)}{R_c^\infty} - 1. \quad (2)$$

$R$  is the Rayleigh number and  $R_c^\infty$  is the critical Rayleigh number for an infinite system. A time-dependent reduced Rayleigh number models an experimental situation in which the temperature difference across the convective cell is a function of time. In the experiments of Meyer and co-workers [5–7] the system is initially prepared below onset ( $\epsilon < 0$ ). The temperature across the cell is then slowly changed such that  $\epsilon > 0$  at the end of the experiment. The constants  $\tau_0$  and  $\xi_0$  are characteristic time and length scales,  $q_c$  is the critical wave number, and  $g_3$  and  $g_5$  are the nonlinear coupling constants. All lengths are measured in units of  $d$ , the cell thickness, and times in units of the thermal diffusion time  $\tau$ . In these experiments,  $d=0.318$  cm and  $\tau=68.745$  s.

For a fluid which is contained between fixed boundaries, and given the parameters of the experiments by Meyer and co-workers, the quantities  $R_c$ ,  $\tau_0$ ,  $\xi_0^2$ ,  $q_c$ , and  $g_3$  are found to be [4, 8, 14]

$$R_c = 1707.762, \quad q_c = 3.117, \quad \xi_0^2 = 0.148,$$

$$\tau_0 = \frac{\text{Pr} + 0.5117}{19.65\text{Pr}}, \quad g_3 = \frac{2}{3} \left[ 0.6995 - \frac{0.0047}{\text{Pr}} + \frac{0.083}{\text{Pr}^2} \right],$$

where Pr is the Prandtl number of the fluid. The coefficient  $g_5$  has not been derived from theory yet. In the calculations to be described below, we will obtain the values of the coefficients  $g_3$  and  $g_5$  by fitting the stationary solutions of the Swift-Hohenberg equation to the stationary current measured experimentally. The function  $f(\mathbf{r}, t)$  is a phenomenological forcing term and will be used to fit the experimental data for the time-dependent convective heat current in the ramping experiment.

We focus on two main causes for the onset of the instability: bulk fluctuations and a thermal diffusivity mismatch at the sidewalls. We model the former by taking  $f(\mathbf{r}, t)$  to be a bulk stochastic field. To model the thermal diffusivity mismatch we can take  $f(\mathbf{r}, t)$  to be either a bulk constant forcing field [8], or impose an inhomogeneous boundary condition on  $\psi$ . In general  $f(\mathbf{r}, t)$  is decomposed into stochastic and deterministic components,

$$f(\mathbf{r}, t) = \eta(\mathbf{r}, t) + \chi(\mathbf{r}), \quad (3)$$

where  $\chi(\mathbf{r})$  is a deterministic forcing field, and  $\eta(\mathbf{r}, t)$  is a stochastic forcing field that satisfies

$$\langle \eta(\mathbf{r}, t) \rangle = 0, \quad (4)$$

$$\langle \eta(\mathbf{r}, t) \eta(\mathbf{r}', t') \rangle = 2F_1 \delta(\mathbf{r} - \mathbf{r}') \delta(t - t').$$

The value of  $F_1$  has been estimated theoretically for the case in which fluctuations are of thermal origin. With

$F_{\text{th}} = (\tilde{F}_{\text{th}}/\tau_0)\tilde{\xi}_0^2$  and  $\tilde{\xi}_0^2 = \xi_0/2q_c$  one obtains [13, 15]

$$\tilde{F}_{\text{th}} = \frac{1}{\tau_0} \frac{k_B T}{\xi_0^2 \text{Pr} R_c^\infty \rho_0 \kappa^2 d}. \quad (5)$$

For water,  $\rho_0=1.0 \text{ g/cm}^3$ ,  $\kappa = 1.471 \times 10^{-3} \text{ cm}^2/\text{s}$ ,  $\text{Pr}=6.0$ . The experiments by Meyer and co-workers that we are investigating were conducted at  $T=298 \text{ K}$ . In the case of rigid-rigid boundary conditions  $\tau_0=0.0552$ . One therefore obtains  $\tilde{F}_{\text{th}}=1.72 \times 10^{-9}$ , or  $F_{\text{th}} = 1.92 \times 10^{-9}$ .

A quantity of primary interest is the dimensionless convective heat current. It can be obtained from the Swift-Hohenberg equation as [8]

$$J^{\text{conv}}(t) = \frac{1}{S} \int d^2 \mathbf{r} \psi(\mathbf{r}, t)^2, \quad (6)$$

where  $S$  is the dimensionless area of the cell. We compare the value of  $J^{\text{conv}}(t)$  obtained from the solution to the Swift-Hohenberg equation to the measured dimensionless convective heat current in Sec. III.

Homogeneous boundary conditions have been used in all the calculations: both  $\psi$  and its normal derivative vanish at all boundaries. We have phenomenologically modeled the effect of a thermal diffusivity mismatch in three different ways. We consider a constant, uniform forcing field in the bulk, a uniform, constant forcing field only in the region adjacent to the boundary, and a random forcing field localized in the region adjacent to the boundary. The first and second model a systematic thermal diffusivity mismatch between the sidewall and the fluid (analogous to the experiments in which a polyethylene sidewall was used); the third models a sidewall with a thermal diffusivity close but not equal to that of water (analogous to the experiments in which a gel sidewall was used). We note, however, that there may not be a consistent way to model lateral heat losses with the stochastic Swift-Hohenberg equation, since the equivalence between this equation and the equations governing fluid motion with due allowance for thermal fluctuations has only been established for bulk systems.

### B. Scaling of the stochastic Swift-Hohenberg equation

In this subsection, we give the details of the procedure used to obtain a numerical solution of Eq. (1). Unscaled variables are unprimed whereas primed variables are the scaled variables used in the numerical calculations. We rescale lengths  $\mathbf{r}$ , time  $t$ , field  $\psi$ , and reduced Rayleigh number  $\epsilon$  by  $\mathbf{r}' = q_c \mathbf{r}$ ,  $t' = \frac{q_c^2 \xi_0^2}{4\tau_0} t$ ,  $\psi' = \frac{2\sqrt{g_3}}{q_c \xi_0} \psi$ ,  $\epsilon' = \frac{4}{q_c^3 \xi_0^3} \epsilon$ . The scaled stochastic Swift-Hohenberg equation becomes

$$\frac{\partial \psi'}{\partial t'} = \left[ \epsilon'(t') - (\nabla'^2 + 1)^2 - \psi'^2 - g_5 \frac{q_c^2 \xi_0^2}{4g_3^2} \psi'^4 \right] \psi' + \frac{8\tau_0 \sqrt{g_3}}{q_c^3 \xi_0^3} f(\mathbf{r}', t'), \quad (7)$$

where  $f(\mathbf{r}', t') = \eta(\mathbf{r}', t') + \chi(\mathbf{r}')$ . The bulk stochastic force satisfies

$$\langle \eta(\mathbf{r}', t') \rangle = 0, \quad (8)$$

$$\langle \eta(\mathbf{r}'_1, t'_1) \eta(\mathbf{r}'_2, t'_2) \rangle = 2F_1 \left( \frac{q_c^2 \xi_0^2}{4\tau_0} \right) q_c^2 \delta^{(2)}(\mathbf{r}'_1 - \mathbf{r}'_2) \times \delta(t'_1 - t'_2).$$

The scaled convective heat current  $J'$  is

$$J' = \frac{1}{S'^2} \int d^2 \mathbf{r}' \psi'^2(\mathbf{r}', t') = \frac{4g_3}{q_c^2 \xi_0^2} J. \quad (9)$$

The experiments were performed in a cylindrical cell of aspect ratio of 20:  $L=20$ , where  $L$  is the diameter of the cell, again in units of the cell thickness. For simplicity, we have considered instead a square cell of side  $L=20$ . We have discretized the cell ( $0 \leq x \leq L$ ,  $0 \leq y \leq L$ ) in evenly spaced intervals  $\Delta x = \Delta y = L/(N+1)$ , with  $N=128$ , so that  $x_i = i\Delta x$ ,  $i=0, \dots, N+1$ , and similarly for  $y_i$ . Therefore the numerical calculation only involves the values of  $\psi$  for nodes  $i, j=1, \dots, N$ . All the others remain equal to zero because of the boundary conditions chosen on  $\psi$ . We use a finite difference scheme to approximate the spatial derivatives in Eq. (10) and explicit integration in time [16]. We have chosen  $N=128$  and  $\Delta x' = \Delta y' = 0.4833$ . Stability of the explicit integration scheme requires that  $\Delta t' \leq \Delta x'/32$ . We have chosen  $\Delta t' = 1.704 \times 10^{-3}$  in all our calculations. With these values of  $\Delta x'$  and  $\Delta t'$ , the amplitude of the fluctuations at short wavelengths are slightly overestimated. For example, the quantity  $\langle \int d\mathbf{r} \psi^2 \rangle$  is 14% higher than the theoretical value for  $\epsilon = -1$  (below onset the Swift-Hohenberg equation can be linearized and this quantity can be evaluated explicitly). Taking  $N=256$  reduced the discrepancy to less than 3%. Nevertheless, no appreciable changes have been observed in  $J(t)$  reported in this paper when  $N=128$  and 256. This is due to the fact that the convective current is dominated by contributions with  $\|\mathbf{q}\| \approx 1$ . Although in some of the cases discussed below we have results for both values of  $N$ , we only show our results for  $N=128$ , for which we have better statistics.

The discretized equation that we have solved is

$$\begin{aligned} & \psi'_i(t' + \Delta t') - \psi'_i(t') \\ &= \Delta t' \left[ \epsilon' - (\nabla'_i + 1)^2 - \psi_i'^2 - g_5 \frac{q_c^2 \xi_0^2}{4g_3^2} \psi_i'^4 \right] \psi'_i \\ &+ \sqrt{2F_1} \frac{4\sqrt{\tau_0 g_3}}{q_c \xi_0^2} \left( \frac{\sqrt{\Delta t'}}{\Delta x'} \right) \eta_i + \frac{8\tau_0 \sqrt{g_3}}{q_c^3 \xi_0^3} \Delta t' \chi_i \end{aligned} \quad (10)$$

where we use the usual four-node discretization of the Laplacian operator and  $\eta_i$  is a Gaussian random variable that satisfies

$$\langle \eta_i \rangle = 0, \quad \langle \eta_i \eta_j \rangle = \delta_{ij}. \quad (11)$$

This variable has been obtained by using the Box-Mueller transformation [17].

### III. RESULTS

The values of most of the coefficients entering Eq. (10) have been obtained from information from the experiments of Meyer and co-workers [6, 7]. In addition, the coefficients  $g_3$  and  $g_5$  have been obtained by fitting the experimentally determined (as a function of  $\epsilon$ ) stationary convective current with the stationary solution of Eq. (10). We have obtained  $g_3 = 0.5441$  and  $g_5 = -0.0414$  [18]. We also use the values of  $\epsilon(t)$  directly measured in the experiments.

We take as initial condition  $\psi'(r', t' = -0.5) = 0$  if  $F_1 \neq 0$ , or a random variable Gaussianly distributed with zero mean and width  $\sqrt{2F_1}4\sqrt{\tau_0 g_3 \Delta T'} / q_c \xi_0^2 \Delta x'$  if  $F_1 = 0$ . Equation (10) is then iterated forward in time up to times comparable to the experiments (approximately 20 000 iterations). The experiment that we have analyzed corresponds to a heating rate  $\beta = 0.27$  with both a plastic and a gel sidewall (Figs. 10 and 12, respectively, in Ref. [7]). The only unknown parameters are the amplitude  $F_1$  and the function  $\chi(r)$ . For any combination of forcing terms, we solve Eq. (10) for different values of  $F_1$  and  $\chi(r)$  until the calculated convective current as a function of time agrees with the experimental curve. We have not made any systematic search of the optimal set of parameters, mainly because the convective heat current does not appear to be very sensitive to small changes in  $F_1$  or  $\chi(r)$ . Once their values have been determined, we perform an ensemble average over 20 independent realizations of the random forces and initial conditions, where appropriate. Finally, we analyze the structure of the emerging roll pattern by directly looking at the values of the function  $\psi'$ .

We now turn to a discussion of our results. First, we show in Fig. 1 the convective heat current  $J(t)$  for several combinations of forcing fields. In all cases, it is possible to find values of the amplitudes of the forcing terms that lead to a good fit to the experimentally measured current; hence this information in itself is not sufficient to discriminate the origin of the instability in the experiments. The corresponding patterns are, however, different. The cases discussed below are illustrative examples of extreme behaviors in terms of the structure and symmetry of the pattern.

Figure 2 shows a sequence of five configurations corresponding to times  $t = -0.37, 1.07, 1.59, 2.12,$  and  $3.03$  with bulk thermal noise  $F_1 = 1.92 \times 10^{-9}$  and constant forcing  $\chi_0 = 1.5$  only at the boundary region ( $\chi = 0$  in the interior of the computational region whereas  $\chi = \chi_0$  on the nodes adjacent to the boundary). A pattern of rolls parallel to the sidewalls emerges near the walls that propagates into the bulk. This behavior is analogous to the experimental case in which a large density plastic was used as the sidewall (Fig. 10 in Ref. [7]), and identical to our earlier results with a uniform bulk forcing (Fig. 2 of Ref. [12]). Note that bulk fluctuations have an amplitude appropriate for thermal fluctuations but are not sufficiently large to destroy the regularity of the pattern.

Figure 3 presents a similar sequence of configurations to Fig. 2, but with a bulk stochastic field with  $F_1 =$

$5.0 \times 10^{-5}$  and  $\chi = 0$ . The pattern observed is similar to that observed in experiments for the case of a gel sidewall (Fig. 12 in Ref. [7]). However, the amplitude  $F_1$  needed to fit the measured convective current is several orders of magnitude larger than that predicted for fluctuations of thermal origin. The value of  $F_1$  found is consistent with earlier estimates obtained from fits to an amplitude equation [7]. In summary, the results obtained in the case of a gel sidewall cannot be explained in terms of thermal fluctuations alone (at least within the context of current models).

Figure 4 presents a sequence of configurations for the same times as Figs. 2 and 3 with  $F_1 = 0$  and  $\chi$  a random function, zero everywhere except at the boundary region. In this case a disordered pattern emerges, similar to that shown in Fig. 3. The main difference with that case is that the pattern of rolls here emerges near the sidewalls and then propagates into the bulk. In the case shown in Fig. 3, the rolls first appear in the bulk. It would be therefore of interest to reanalyze the experiments involving a gel sidewall to ascertain, if possible, the location of the region where the rolls first appear after the instability, and thus rule out any possible sidewall influence on the pattern.

Finally, Fig. 5 presents a sequence of configurations at the same times as in the previous figures. In this case,

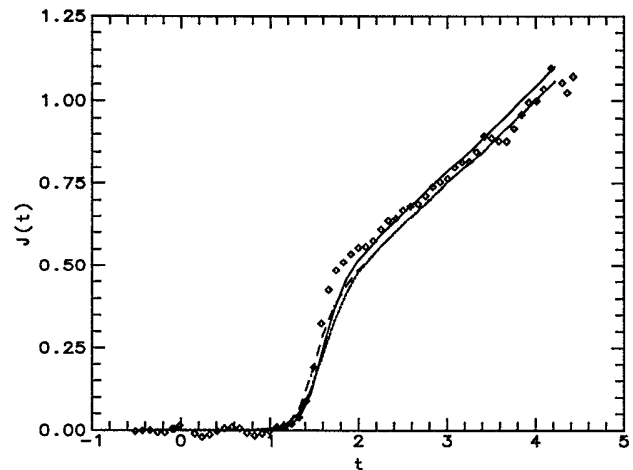
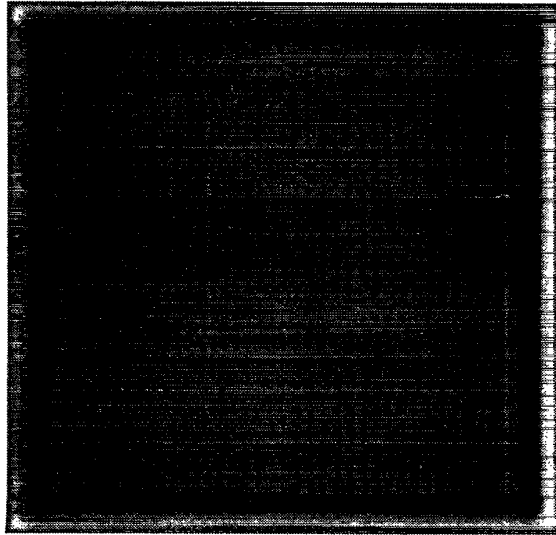
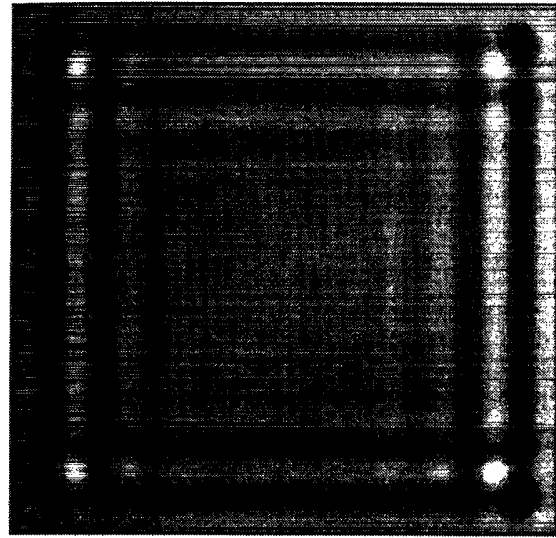


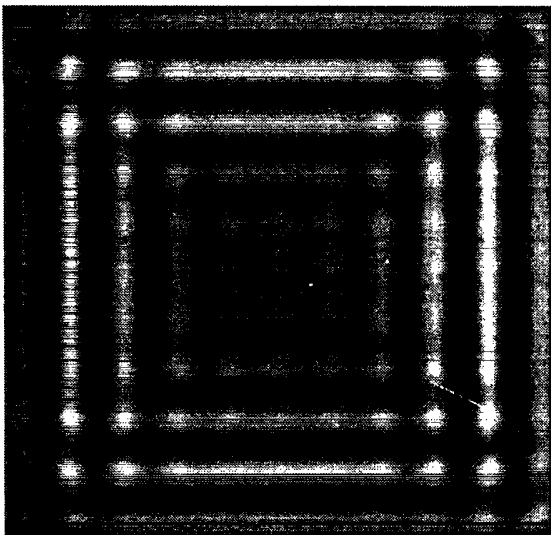
FIG. 1. (a) Experimentally obtained convective heat current, after Meyer and co-workers [5, 6] ( $\diamond$ ). The fluid used is water and the ramp rate for the temperature difference across the cell is  $\beta = 26$ . The solid line corresponds to the convective current obtained from the solution of the Swift-Hohenberg equation with a bulk stochastic field of amplitude  $F_1 = 1.92 \times 10^{-9}$  and a deterministic forcing field confined to the sidewall region of amplitude  $\chi_0 = 1.5$ . The results for  $J(t)$  are averages over 20 independent realizations. A particular sequence of configurations of the field  $\psi'$  is shown in Fig. 2. The dashed line corresponds to the convective heat current obtained with a bulk stochastic field alone of amplitude  $F_1 = 5 \times 10^{-5}$ , again averaged over 20 independent realizations. A particular sequence of configurations of the field  $\psi'$  is shown in Fig. 3. The dotted line is the convective heat current corresponding to a random field confined to the boundary region.



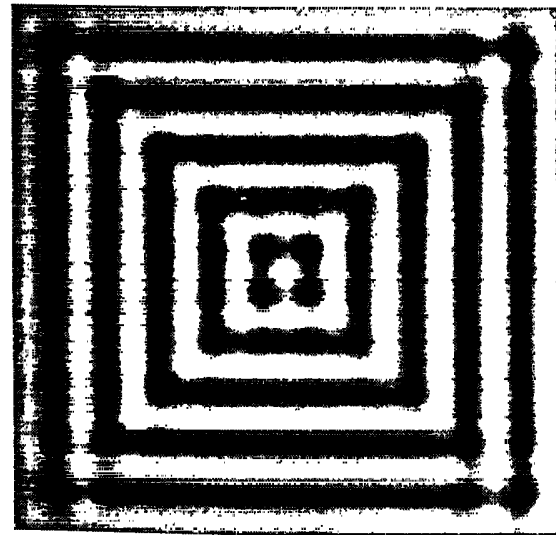
(a)



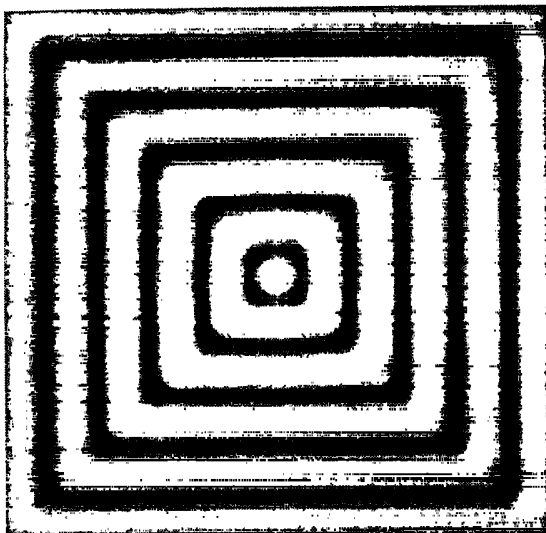
(b)



(c)

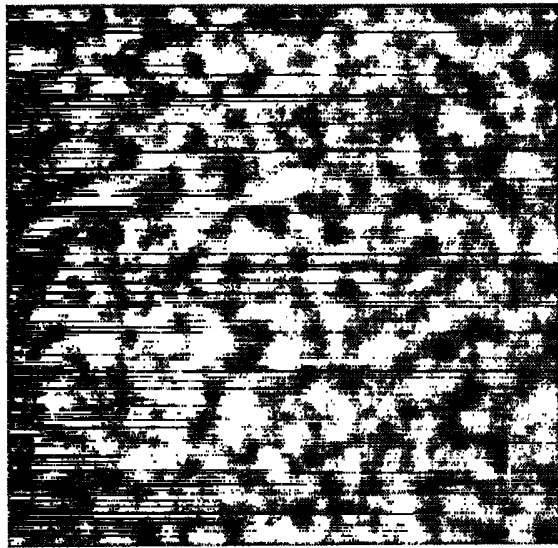


(d)

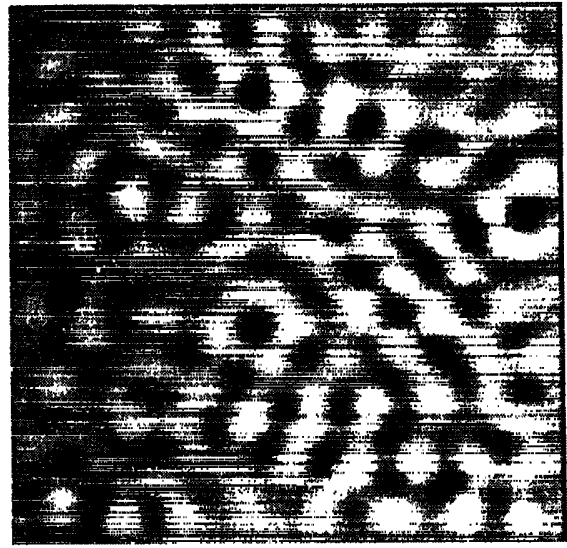


(e)

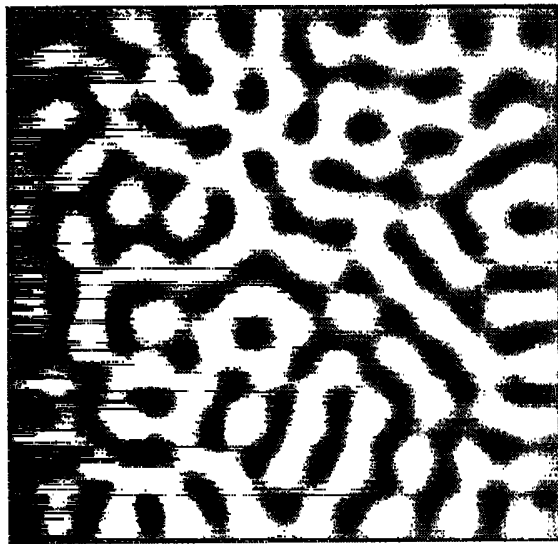
FIG. 2. Sequence of configurations at times  $t = -0.37$ , 1.07, 1.59, 2.12, and 3.03. The forcing fields chosen are a bulk stochastic field with  $F_1 = 1.92 \times 10^{-9}$ , the value predicted by hydrodynamic fluctuation theory, and a deterministic forcing confined to the sidewall region of amplitude  $\chi_0 = 1.5$ . The corresponding convective current is shown in Fig. 1. The salient features of this case include a pattern of rolls that reflects the symmetry of the sidewalls and the fact that convection first appears in the region near the sidewalls. Both observations are consistent with the experiments performed in a convective cell with a polyethylene sidewall.



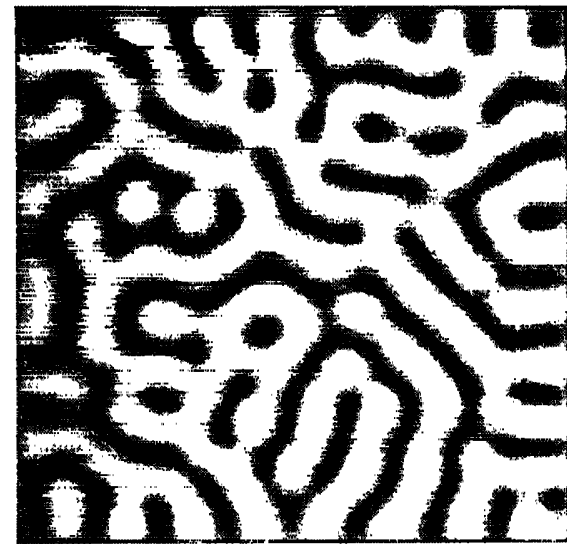
(a)



(b)



(c)



(d)



(e)

FIG. 3. Sequence of configurations at times  $t = -0.37$ , 1.07, 1.59, 2.12, and 3.03. The forcing term is purely stochastic with  $F_1 = 5 \times 10^{-5}$ . The corresponding convective current is shown in Fig. 1. The roll pattern appears to be disordered for all times, appears in the interior of the region and differs from run to run (for different realizations of the stochastic field). These results are consistent with the experiments performed in a convective cell with a gel sidewall. The value of  $F_1$  obtained, however, is much larger than that predicted by classical fluctuation theory.

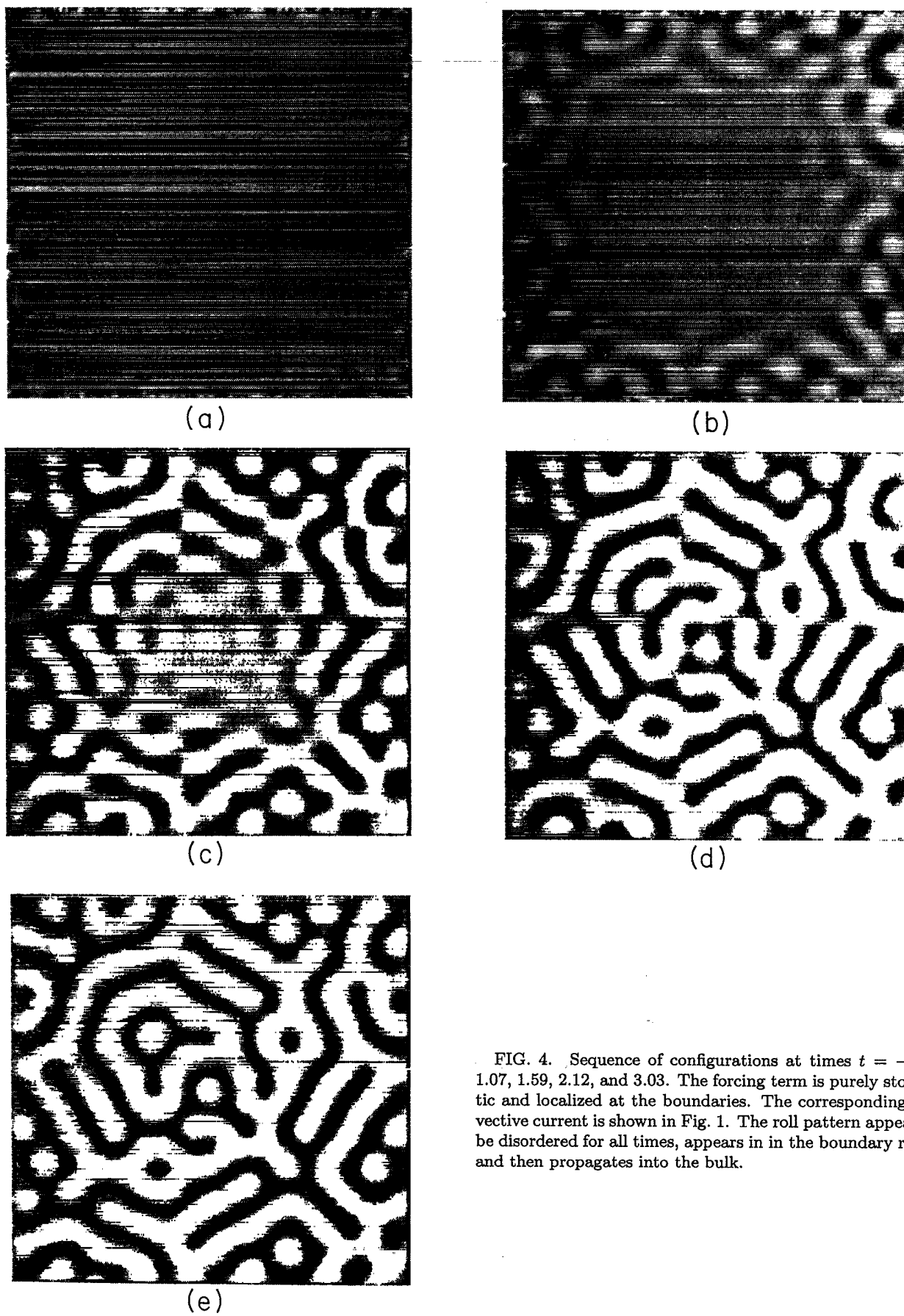
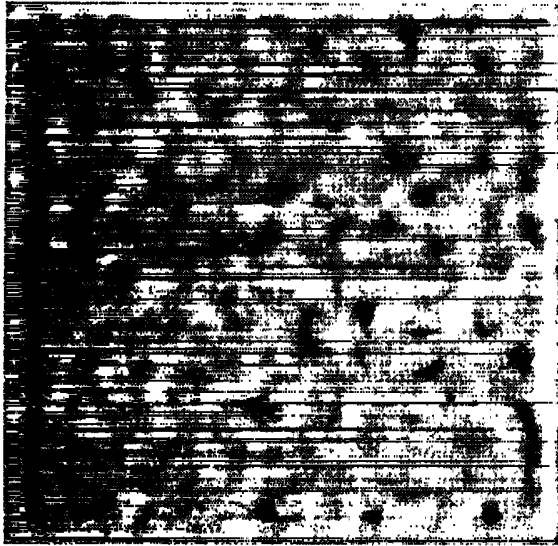
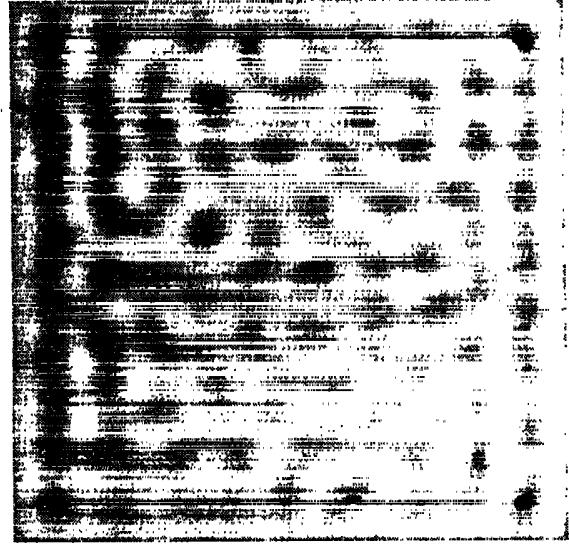


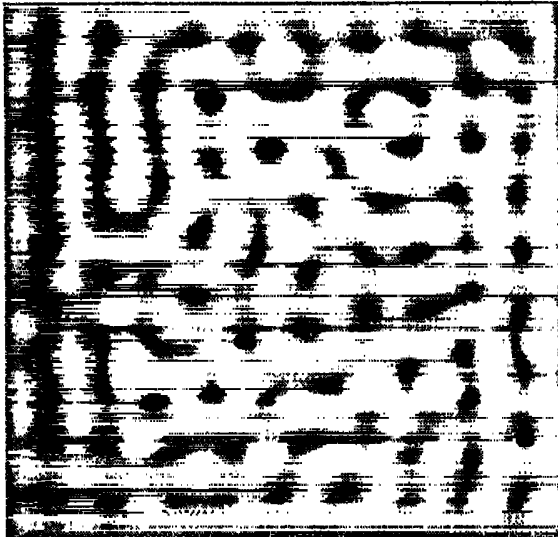
FIG. 4. Sequence of configurations at times  $t = -0.37, 1.07, 1.59, 2.12,$  and  $3.03$ . The forcing term is purely stochastic and localized at the boundaries. The corresponding convective current is shown in Fig. 1. The roll pattern appears to be disordered for all times, appears in the boundary region and then propagates into the bulk.



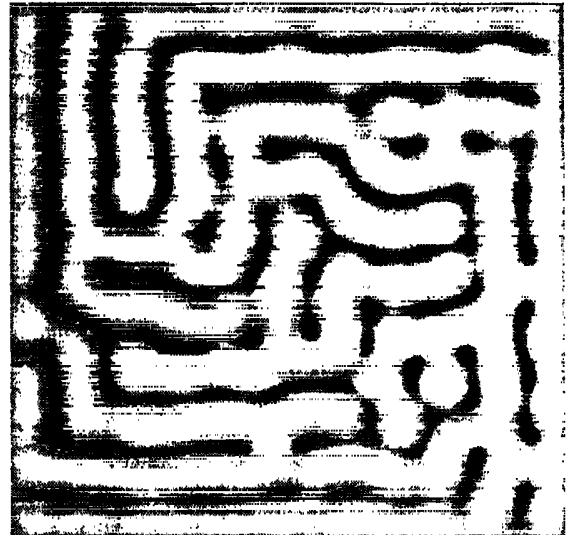
(a)



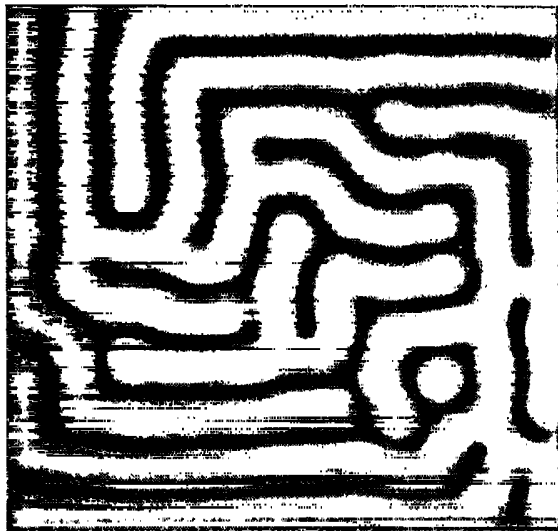
(b)



(c)



(d)



(e)

FIG. 5. Sequence of configurations at times  $t = -0.37$ , 1.07, 1.59, 2.12, and 3.03. The forcing fields chosen are a bulk stochastic field with  $F_1 = 1.29 \times 10^{-5}$  and a deterministic forcing confined to the sidewall region of amplitude  $\chi_0 = 1.5$ . The corresponding convective current is very similar to those shown in Fig. 1.

we have used a bulk noise amplitude similar to that used to fit the experiments conducted with a gel sidewall and added the same deterministic sidewall forcing field used for the case of a plastic sidewall:  $F_1 = 1.29 \times 10^{-5}$  and  $\chi = 1.5$ . The convective current obtained is very similar to those shown in Fig. 1. It is apparent from Fig. 5 that the emerging pattern is not completely ordered and that it contains defects, with the rolls on either side of the defects tending to terminate more or less perpendicular to the walls. The defects did not heal to a symmetric pattern over the time interval studied. Therefore, the pattern is not completely determined by the geometry of the sidewall (compare Figs. 2 and 5), implying that the gel sidewall itself directly (or indirectly) may have played an important role in generating the large apparent noise seen in the gel sidewall experiment. The reason is the following: the only difference between the two sets of experiments is the sidewall, one is made of a plastic material and the other is made of a gel. If the large bulk noise observed in the experiment using a gel sidewall were not due to the sidewall, then bulk noise of the same amplitude should be present in the plastic sidewall experiment as well. However, adding a bulk noise of that amplitude to the case of a plastic sidewall leads to a considerably more disordered pattern than is observed experimentally (Fig. 5). We therefore conclude that the large amplitude needed to fit the experiments performed in the case of a gel sidewall probably originates from the sidewall itself and not from underlying thermal fluctuations in the fluid.

#### IV. CONCLUSIONS

Our results indicate that the stochastic Swift-Hohenberg equation accurately describes the convective heat current during a ramping experiment in a Rayleigh-Bénard cell with only one adjustable parameter, the amplitude of the forcing field that triggers the instability. The equation further allows the study of the convective pattern that results as a function of the forcing mechanism. A number of different forcing mechanisms, both deterministic and random in nature, can be invoked to explain the origin of the instability. We have explored a number of such possibilities and determined the intensity of the various contributions so that the calculated convective current would be equal to the convective current measured in the experiments. We conclude that a deterministic forcing field which is either a uniform bulk field or a localized sidewall forcing allows a fit to the measured convective current for the case in which there is a thermal diffusivity mismatch at the sidewalls. The pattern observed is comprised of straight rolls parallel to the boundaries, in agreement with experimental observations.

We further conclude that thermal fluctuations alone are not sufficient to reproduce the onset time observed in the experiments. The amplitude of the random bulk fluctuations needed to fit the convective heat current measured experimentally is  $F_1 = 5 \times 10^{-5}$ , in contrast

with the prediction of hydrodynamic fluctuation theory,  $F_{th} = 1.92 \times 10^{-9}$ . The pattern observed in the case of a large random forcing, however, appears to be qualitatively similar to the pattern observed in the experiments that use a gel sidewall.

To further elucidate the origin of the large amplitude of the stochastic contribution needed to fit the experiments involving a gel sidewall, we have explored a number of different forcing mechanisms and of combinations among them. We have studied a random, time-dependent forcing field localized at the sidewall (Fig. 4), and a combination of bulk stochastic forcing and deterministic sidewall forcing (Fig. 5). In the former case, a random or cellular pattern develops, starting at the boundary and propagating into the bulk. This does not seem to be the case in the experiments. In the latter case, a disordered pattern with defects appears throughout the cell. This differs from the observation of a regular pattern with the symmetry of the container in the experiments that involve a plastic sidewall. This suggests that the gel sidewall itself is likely to be responsible for the large noise amplitude needed to fit the experiments. Of course, we cannot rule out the existence of some other unknown mechanism that may lead to a similar effect.

Finally, we have not been able to obtain a cellular pattern with a combination of forcings that would simultaneously fulfill all of the following requirements: (a)  $F_1 = F_{th}$ , (b) cellular patterns without marked relationship to the geometry of the cells, and (c) different patterns from run to run (i.e., for different sequences of the random, time-dependent bulk forcing that models thermal fluctuations).

In summary, our analysis based on the Swift-Hohenberg equation, with the parameters appropriate to the experiments of Meyer and co-workers, suggests that even under the most stringent experimental conditions aiming at eliminating the influence on convection of the sidewalls of the experimental cell, the bifurcation observed is imperfect and not triggered by fluctuations of thermal origin.

#### ACKNOWLEDGMENTS

We would like to thank G. Ahlers and P.C. Hohenberg for suggesting the numerical investigation of the stochastic Swift-Hohenberg equation and G. Ahlers, D. Cannell, C. Meyer, and P.C. Hohenberg for many stimulating conversations and comments. We also thank H. Greenside for useful suggestions concerning the numerical code. This work was supported in part by the National Science Foundation under Grant No. DMR-9100245. This work is also supported in part by the Supercomputer Computations Research Institute, which is partially funded by the U.S. Department of Energy Contract No. DE-FC05-85ER25000. All the calculations reported here have been performed on the 64k-node Connection Machine at the Supercomputer Computations Research Institute. We also thank Jim Hudgens of SCRI for his assistance with the graphics packages used to analyze the data.

- [1] L.D. Landau and E.M. Lifshitz, *Fluid Mechanics* (Addison-Wesley, Reading, MA, 1959), Chap. XVII.
- [2] R. Graham, *Phys. Rev. A* **10**, 1762 (1974).
- [3] J. Swift and P.C. Hohenberg, *Phys. Rev. A* **15**, 319 (1977).
- [4] J. Swift and P.C. Hohenberg (unpublished).
- [5] C.W. Meyer, G. Ahlers, and D.S. Cannell, *Phys. Rev. Lett.* **59**, 1577 (1987).
- [6] C.W. Meyer, Ph.D. thesis, University of California, Santa Barbara, 1988.
- [7] C.W. Meyer, G. Ahlers, and D.S. Cannell, *Phys. Rev. A* **44**, 2514 (1991).
- [8] G. Ahlers, M.C. Cross, P.C. Hohenberg, and S. Safran, *J. Fluid Mech.* **110**, 297 (1981); M.C. Cross, P.C. Hohenberg, and M. Lücke, *ibid.* **136**, 269 (1983).
- [9] M.C. Cross, *Phys. Fluids* **23**, 1727 (1980); *Phys. Rev. A* **25**, 1065 (1982); **27**, 490 (1983).
- [10] M.C. Cross, *Phys. Fluids* **25**, 936 (1982).
- [11] H.S. Greenside and W.M. Coughran, Jr., *Phys. Rev. Lett.* **49**, 726 (1982); *Phys. Rev. A* **30**, 398 (1984); H.S. Greenside and M.C. Cross, *ibid.* **31**, 2492 (1985).
- [12] H.W. Xi, J. Viñals, and J.D. Gunton, *Physica* **177**, 356 (1991).
- [13] J.B. Swift, P.C. Hohenberg, and G. Ahlers, *Phys. Rev. A* **43**, 6572 (1991).
- [14] A. Schluter, D. Lortz, and F. Busse, *J. Fluid Mech.* **23**, 129 (1965).
- [15] H. van Beijeren and E.G.D. Cohen, *J. Stat. Phys.* **53**, 77 (1988).
- [16] J. Viñals, E. Hernández García, R. Toral, and M. San Miguel, *Phys. Rev. A* **44**, 1123 (1991).
- [17] G. Dahlquist and A. Björk, *Numerical Methods* (Prentice-Hall, Engelwood Cliffs, NJ, 1974).
- [18] The value that we have obtained for  $g_3$  is approximately equal to 2/3 of the value given in Ref. [7]. The factor of 2/3 is due to the fact that we have fitted the stationary solution of Eq. (1) to the stationary convective current measured experimentally, whereas in Ref. [7], an amplitude equation was used instead. The value of the coefficient of the cubic term that appears in the Swift-Hohenberg equation equals 2/3 the same coefficient in the amplitude equation.